Development of Multifunctional Bio-based Cotton Composite

Emine Altınkaya‡ [iD] *0000-0002-5652-3156

‡ Manisa Celal Bayar University / Department of Bioengineering / Faculty of Engineering, Muradiye, Manisa, Turkey

Corresponding Author: Emine Altınkaya, emine.altinkaya@cbu.edu.tr

ABSTRACT

In this study, the production and characterization studies of clay-chitosan based composites were investigated. The composite products were characterized by Scanning Electron Microscopy, Thermo Gravimetric Analysis, and Fourier Transform Infrared Spectroscopy. Besides antibacterial effect of the composites against S. Aureus and K. Pneumonia and dye adsorption properties were investigated. The effects of contact time, ionic strength, pH, and temperature on removal of remazol blue were investigated for the adsorption studies. The comparison was performed based on the characterization results of treated and untreated cottons. It was revealed that the one-step process of clay-chitosan-based fabrics gave significantly good properties to fabrics. These improved properties expressed the dyeing free-salt, antibacterial activity, and enhanced dyeability (dye adsorption capacity) of cotton. Consequently dyeability of the cottons was increased with the treatments. These treatments can be used in textile industry for the free salt dyeing which is a desirable property for the cotton in addition to the gained antibacterial activity. As a result, clay-chitosan composites can be considered as a hopeful composite for the multifunctional finishing textiles.

1. INTRODUCTION

Textile finishing is an important stage in making textile products suitable for use. The processes involved in textile finishing are the steps where the most water and energy consumption is made. Wastewater produced by textile processing plants leads to serious water and air pollution. With increasing environmental awareness, environmentally friendly and sustainable products and methods are preferred in textile goods production. Modern consumers ' demand for both aesthetic and multi-functional products is increasing day by day. UV protection, antibacterial, water-oil repellency, self-cleaning properties can be gained to the fabric by using finishing agents. Organic, inorganic, and composite materials can be used in the finishing process. In the textile sector, environmentally friendly processes are needed that can meet the demands of consumers and save water and energy. In recent years, traditional methods have been replaced by nanotechnology, biopolymers, enzyme, chemical products obtained from natural sources, plasma applications [1, 2].

Dyes are utilized in various fields such as textiles, cosmetics, plastic, leather, etc., for coloring the products [3]. Factories discharge large amounts of environmentally hazardous toxic waste, mostly of textile dye and finishing salts. The hydroxyl group in cellulose is negatively charged upon contact with water. The dyes used for cotton are generally anionic. The negative charges of cotton repulse the dye. And so the repulsion of negative charges decreases the dyeing of cotton. A great quantity of electrolyte is used to recovery the affinity between anionic dye and negative charged cotton [4]. But the release of these electrolytes into nature causes great damage to the environment. Textile

To cite this article: Altınkaya E. 2021. Development of multifunctional bio-based cotton composite *Tekstil ve Konfeksiyon* 31(4), 264-273.

dyes and finishing salts used in fabric dyeing account for 17-20 percent of water pollution [5]. The pollutions (finishing salts, textile dyes) are ecotoxic, and give a huge hazardous to environment, human, animals, etc. The pollution should remove from waste water. [6]. Salt-free dyeing is important for the textile industry due to being an ecofriendly method [4]. The dyeability of fabric can be enhanced by modification or cationization of the fabric surface. The fabric surface can be cationized with chitosan and enhanced the dyeability of fabric. These processes applied to the fabric are classified as salt free dyeing [7].

Various techniques such as chemical adsorption, oxidation, ozonation, coagulation are utilized for the elimination of organic and inorganics impurities from drain water [8]. Adsorption is the most using method due to get rid of dye contamination from drain water. Adsorbent materials can be classified into five category based on their ability: plant waste, fruit waste, natural inorganic materials, waste of industry, and bioadsorbents [8]. Clays as a natural inorganic material are widely used in adsorption studies [9].

Clays are natural materials with high surface area. Clays have many usage areas due to their mechanical, thermal, and unique properties. KSF is a natural clay mineral. KSF has no adverse effects on humans and animals [10]. Montmorillonite (KSF) has a large adsorption capacity thanks to smectite group in structure [11]. The use of additives such as KSF can be considered a universal method to increase adsorption capacity [12]. Coating the cotton with KSF can help to dye with a small amount of paint thanks to the adsorption capacity of KSF. KSF is an effective reinforcement material in enhancing the antimicrobial effect [12].

Chitosan, deacetylated chitin, is inexpensive, abundant, non-toxic, biocompatible, and eco-friendly material [13]. Chitosan is an abundant biopolymer in the world that makes chitosan economic [14]. And also chitosan is attractive biopolymer due to having antibacterial and adsorption properties. It is used for dye removal from wastewater [15]. The polycationic structure enhances the dye adsorption capacity of chitosan [6, 11, 16]. Chitosan-inorganic composite have wide application areas (drug release, packaging material, biodegradable materials, dye removal, electrochemical sensor) [17]. Chitosan-inorganic composites can be used to obtain multifunctional properties [18].

In this study, it was aimed to fabricate the bio-based multi-functional composites material via using invaluable properties of chitosan and KSF. It was aimed to gain the fabric dye adsorption capacity, antibacterial properties, free salt dyeability and effective dyeing with a small amount of paint. For these purpose cotton was treated with chitosan, KSF and dihydroxy ethylene urea (MDEU) in one step process.

Novelties of this study are "gain antibacterial properties to the cotton thanks to the natural properties of chitosan and KSF", "enhance the affinity between cotton and dye thanks to the properties of clay and chitosan," and "obtain eco-friendly, economic, and effective fabric dyeing without using "finishing salts" by improving the affinity between fabric and dyestuff".

The dye [Remazol Blue (RB)] adsorption and antibacterial feature of cotton samples were studied. Then the samples were characterized via Scanning Electron Microscopy (SEM), Thermo Gravimetric Analysis (TGA) and Fourier Transform Infrared Spectroscopy (FTIR) instruments.

2. MATERIALS AND METHODS

2.1. Materials

100 % cotton fabric (153 g/m^2) was utilized in this study. The cotton was bleached and scoured woven. Chitosan (highly viscous, average MW: 500000-700000 gm^{-1}, degree of deacetylation: 75–85 %), MDEU, and glacial acetic acid (CAS Number: 64-19-7) were supplied from Fluka, Huntsman, and Sigma- Aldrich, respectively. KSF MMT (surface area of 20-40 m^2/g) was supplied from Fluka. Chemical composition of KSF is 3.0% MgO, 18.0% Al_2O_3, 55.0% SiO_2, %3.0 CaO, 1.5% K_2O, 4.0% Fe_2O_3, 5.0% Sulphate, <0.5% Na_2O, and 10.0% loss on ignition.

2.2. Fabrication of Sample

2.2.1 Fabrication of Cot-KSF

KSF mixture was prepared for cotton padding. For this purpose 2% KSF mixture was prepared overnight to swell the clay. The cotton was padded in swelled 2% KSF mixture and squeezed. The wet cotton was dried for 5 min and cured for 3 min at 80 °C and 120 °C, respectively.

2.2.2 Fabrication of Cot-KSF-chi

The 2% KSF mixture was prepared overnight to swell the clay. Chitosan solution (2%) was prepared with 2% acetic acid solution. The chitosan solution was added in swelled KSF mixture and mixed for 6h at 60 °C. Cotton was padded in the mixture (KSF-chi) and wringed. The wet cotton was dried for 5 min and cured for 3 min at 80 °C and 120 °C, respectively.

2.2.3 Fabrication of Cot-KSF-chi-MDEU

The 2% KSF mixture was prepared overnight to swell the clay. MDEU (150 kg m^{-3}) was added to the swelled KSF mixture. Chitosan solution (2%) was prepared with 2% acetic acid solution. The chitosan solution was added in the KSF-MDEU mixture and mixed for 6h at 60 °C. Cotton was padded in the mixture (KSF-chi-MDEU) and squeezed. The wet cotton was dried for 5 min and cured for 3 min at 80 °C and 120 °C, respectively.

2.3. Characterization of Samples

2.3.1. FTIR analysis

The describing of functional groups in sample structure was investigated by Fourier Transform Infrared (FTIR) analysis.

ATR-Perkin Elmer Spectrum BX-II model FTIR was used for investigation [19].

2.3.2. Scanning electron microscopy (SEM)

The samples morphologies were investigated by scanning electron microscope (FEI Quanta FEG 250 SEM). The accelerating voltage was 5-12 kV. The fabricated samples were prepared for SEM analysis by coating the surface with gold [19].

2.3.3 Thermo gravimetric analysis (TGA)

The Thermo Gravimetric Analysis of samples was performed with Perkin Elmer Diamond TG/DTA. Samples were analyzed by heating (30 to 600 °C) under nitrogen flow (10 °C min^{-1}) [19].

2.4. Adsorption Study

For this study, 25 mL Remazol Blue solution was prepared in different initial concentrations. 0.1 g of treated and untreated cotton fabrics (1 cm x 1 cm) were used due to adsorption studies. The cotton fabric was removed from Remazol Blue solution when the equilibrium was achieved. The latest concentration of Remazol Blue solution was investigated by UV- visible spectrophotometer (Shimadzu, model UV 1601) at 604 nm. The adsorbed (at equilibrium) dye amount q_e (mg/g) was calculated according to the equation:

$$q_e = \frac{C_0 - C_e}{m} V \tag{1}$$

where C_o (mg/L) is the beginning concentration of Remazol blue, V indicates the solution volume (L), m (g) indicates the cotton fabric mass, and C_e (mg/L) is the equilibrium concentration of Remazol Blue solution. The adsorption studies were performed in a thermostat shaking water bath (150 rpm) at different temperatures of 298, 308, 318 and 338 K [20].

2.5. Kinetic Study

Kinetic studies were performed by using 25 mL RB solution and 0.1 g untreated and treated cotton fabric. The cotton was put into the RB solution and mechanically agitated at various temperatures. The adsorbed dye at certain interval of time was determined with UV- visible spectrophotometer [20].

2.6. Effect of pH

The impact of beginning pH on adsorption of RB on treated and untreated cotton fabric was investigated at various pH values (4–10).

The initial pH values were adjusted by 0.1 M NaOH and 0.1 M HCl. 0,1g cotton was used in this study. The study

conditions; RB concentration was 15 ppm, shaking time was 90 min, temperature was 298 K [20].

2.7. Effect of Ionic Strength

Effect of ionic strength on RB adsorptions of cotton was performed using various concentrations of NaCl (12-50g/L). 0,1g cotton was used in this study. The study conditions; RB concentration was 18 ppm, shaking time was 90 min, temperature was 298 K [20].

2.8. Antibacterial Activity

The antibacterial activity of fabricated samples was investigated against Gram-negative bacteria (*Klebsiella pneumonia*-ATCC 4352) and Gram-positive bacterium (*Staphylococcus aureus* - ATCC 6538) according to AATCC Test Method 100-2007. The reduction of bacteria was evaluated in "0" and "24" h. 1 mL diluted bacteria (1– 2×10^5 CFU mL^{-1}) was added on fabric samples (diameter: 4,8cm). The fabric samples were incubated at 37 °C for "0" and "24" h. The incubated fabric was put in 100 mL distilled water and shook for 1 min. 1µL from this solution was put on agar and incubated at 37 °C for 24 h [19].

The following equation gives the percentage reduction of bacteria (R) by the cotton samples:

$$R = 100 * \frac{B - A}{B} \tag{2}$$

where A is the number of bacteria of "24"h treated, B is the number of bacteria of "0"h treated samples [13]. Antimicrobial activity of Cot-KSF, Cot-KSF-chi, and Cot-KSF-chi-MDEU was investigated.

3. RESULTS AND DISCUSSION

3.1. Characterization of Samples

3.1.1. FTIR analysis

Figure 1 shows the FTIR analysis of untreated cotton, cot-KSF, cot-KSF-chi, and cot-KSF-chi-MDEU. The samples exhibited similar spectra as exhibited in Figure 1. The broad band at around 3350 cm^{-1} indicated the OH stretching that overlapped the N-H stretching vibration. The broad band at around 3350 cm^{-1} was OH stretching for untreated cotton and cot-KSF while N-H stretching vibration for cot-KSF-chi, and cot-KSF-chi-MDEU. The peaks around 2920-2925 cm^{-1} indicate the C-H stretching vibrations and also indicate the C-H stretching vibration in –CH$_2$ and –CH$_3$ of chitosan. The small peak at around 1320, 1570, and 1670cm^{-1} was indicated the C-N (amide III) stretching, N-H (amide II), and carbonyl group (amide I) vibrations, respectively. The peak at around 1058 cm^{-1} the peak was shown in all samples but the intensity of the peak was decreased for cot-KSF-chi, and cot-KSF-chi-MDEU. The decrease in intensity of peak can be explained with the interaction Si-O-Chitosan bonding [21-24].
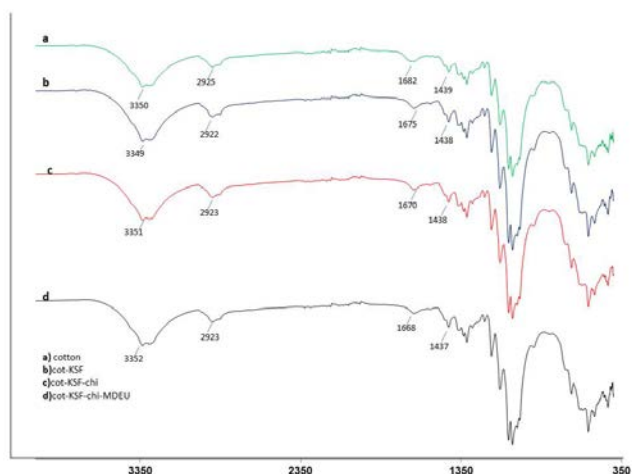
Figure 1. FTIR Analysis of untreated cotton, cot-KSF, cot-KSF-chi, and cot-KSF-chi-MDEU.

3.1.2. Scanning electron microscopy (SEM)

The SEM analysis of untreated cotton, cot-KSF, cot-KSF-chi, and cot-KSF-chi-MDEU was indicated in Figure 2 at 5000x magnifications. Figure 2a shows the untreated cotton surface. The fiber of untreated cotton can be seen clearly. The KSF particles are seen on the cot-KSF sample indicated in Fig.2b. The coated chitosan and KSF on cotton can be seen in Fig.2c. as can be seen in Fig 2c and 2d chitosan filled the gap between the fibers. MDEU was used as crosslinker agent for cot-KSF-chi-MDEU and so the chitosan and KSF hang on to the cotton surface.
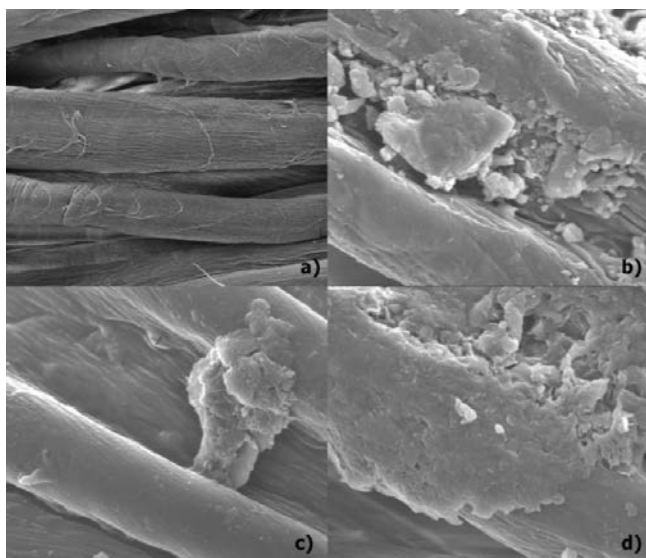
Figure 2. SEM figure of a) untreated cotton, b) cot-KSF, c) cot-KSF-chi, and d) cot-KSF-chi-MDEU.

3.1.3 Thermo gravimetric analysis (TGA)

The TGA curves of samples were given in Figure 3. The decomposition temperature of untreated cotton, Cot-KSF, Cot-KSF-chi, and Cot- KSF -chi-MDEU was investigated as 369, 362, 351, and 351 °C, respectively. The decomposition temperature of untreated cotton was investigated at around 369°C as reported in Gaan and Sun study [25]. The max. decomposition temperature was

decreased from 369 to 351°C for untreated cotton, Cot-KSF, Cot- KSF -chi, and Cot- KSF -chi-MDEU. The max degradation temperature of cellulose was decreased after treatments. The decrease in max decomposition temperature can be due to damage of strong H bonds in cellulose. The materials in the structure of samples can be lead to damage of H bonds in cellulose. Shanks and Ouajai reported that cellulose which has greater crystalline structure decompose at higher temperature [26]. And also Altınışık et al. reported that the CI (crystallinity index) of cellulose was decreased after treatments and the lower CI led to the decrease in decomposition temperature [19].
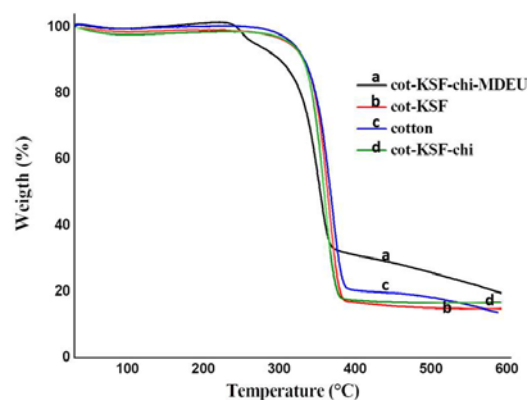
Figure 3. TG curves of samples untreated cotton (c), cot-KSF (b), cot-KSF-chi (d), and cot-KSF-chi-MDEU (a).

Table 1. Results of thermogravimetric analysis.

Sample	T (°C)	Mass loss %
Cotton	369	80
Cot- KSF	362	85
Cot- KSF -chi	351	83
Cot- KSF -chi-MDEU	351	69

3.2. Effect of pH

Investigation of the impact of pH on RB adsorption on the treated and untreated cotton fabric was investigated at beginning dye concentration of 15mg/L with an amount of treated and untreated cotton fabric of 0.1 g/25 mL for equilibrium time of 90 min at 25 °C.

The results of RB dye adsorption in the pH range 4–10 were given in Fig. 4. The adsorption of RB on the treated and untreated cotton fabric, q_e (mg/g), decreased as the acidity decreased. The increase in acidity makes the adsorbent surface positively charged, thereby leading to an increase in adsorption of RB on adsorbent. Generally the removal of anionic dyes increase as the pH value increased while for cationic dyes decreased [3, 27].

Clay has hydrated sodium, silanol groups (SiOH) on the surface, and R-NH_3^+ groups (chitosan) in the interlayer area [4, 28]. The decrease in pH level gave rise to protonation of -NH_2 group (-NH_3^+) on the surface and ionization of SiOH. At low pH values, protonation of clay surface enhanced the electrostatic interaction. On the other hand, as the pH

values increased (more basic) the surface of clay was deprotonated. Deprotonation of the surface made difficult the access of negatively charged dye molecules to surface adsorption sites. The results exhibited the interaction between the adsorbent and dye molecules. The interactions were hydrogen bonding and the van der Waals interactions [29].

Figure 4 shows that the max adsorption capacity was evaluated at pH 4 for treated and untreated cotton. At pH 4 the optimal adsorption capacity (removal of RB dye) was reached due to an electrostatic interaction between anionic RB dye and the protonated sample surface. At higher pH levels dye adsorption capacity was decreased result of the competition between OH^- ions and anionic RB dye molecules [29].
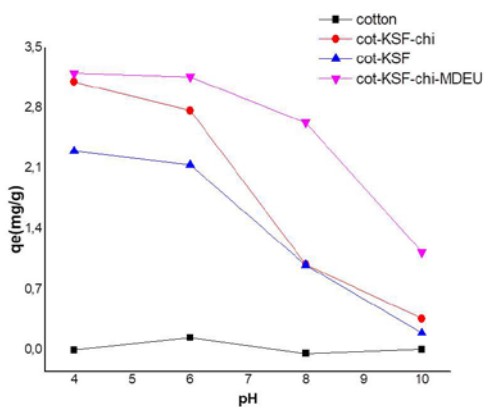
Figure 4. Impact of pH on dye adsorption of cotton, Cot- KSF, Cot- KSF -chi, and Cot- KSF -chi-MDEU.

3.3. Effect of Ionic Strength

The impact of salt concentration on dye removal was investigated. The dye solution was adjusted pH 4 where is the max adsorption observed. The attraction between adsorbate ions and adsorbent surface decreased from 0 (g/L) to 50 (g/L) salt concentration. So that q_e (mg/g) of adsorbent (treated cotton samples) decreased [30-32]. As indicated in Fig. 5, the adsorption capacities of treated samples were decreased while untreated cotton's was increased. The increase in ionic strength enhanced the electrostatic attraction between untreated cotton and RB.
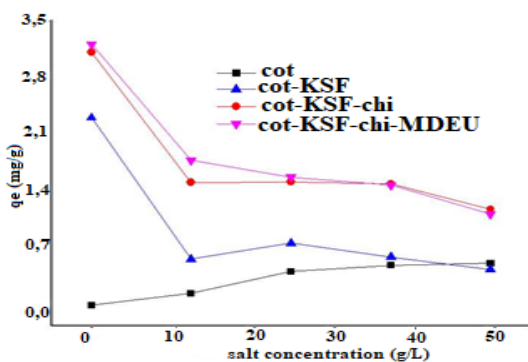
Figure 5. The impact of ionic strength on adsorption capacity of cotton, Cot- KSF, Cot- KSF -chi, and Cot- KSF -chi-MDEU.

3.4. Adsorption Isotherm

Dubinin-Radushkecich, Langmuir, Brunauer–Emmett–Teller, and Freundlich isotherm equations were used to investigate the equilibrium character of adsorption.

Langmuir adsorption supposes that adsorption takes place at homogeneous active sites on the adsorbent and adsorbed molecules. Langmuir isotherm is proper for monolayer adsorption on a homogeneous surface. The Langmuir isotherm equation with linearized form is indicated below [20, 33]:

$$\frac{C_e}{q_e} = \frac{1}{q_m L} + \frac{C_e}{q_m} \tag{3}$$

where C_e indicates the equilibrium concentration (mgL^{-1}) of dye in solution, q_e (mgg^{-1}) is the adsorbed dye per unit weight at equilibrium, q_m indicates the monolayer adsorption capacity (mgg^{-1}), L is the constant of Langmuir related to adsorption energy.

The fundamental properties of Langmuir isotherm may be explained in terms of dimensionless constant separation factor R_L [34]:

$$R_L = \frac{1}{1 + b.C_0} \tag{4}$$

where b indicates Langmuir constant, C_0 indicates beginning dye concentration (mgL^{-1}). The R_L explains the type of isotherm to be linear ($R_L= 1$), irreversible ($R_L=0$), favorable ($0<R_L<1$), and unfavorable ($R_L>1$). The values related to Langmuir isotherms are given in Table 2. The given RL values are between 0 and 1. According to RL values indicated in Table 2, the adsorption is favorable.

The Freundlich isotherm is an experimental equation to describe the adsorption on the heterogeneous surfaces as well as multilayer sorption. The Freundlich isotherm equation is given below with linearized form [35]:

$$log q_e = log K_f + \frac{1}{n_f}.log Ce \tag{5}$$

where the Kf (mgg^{-1}) and nf are the constant of Freundlich isotherm. Kf indicates adsorption capacity and nf represent adsorption intensity. Ce is the remnant dye concentration in solution; qe is the adsorbed dye on adsorbent at equilibrium. The calculated values of

Freundlich isotherms are given in Table 2. Given correlation coefficient (R^2) values depict that Freundlich isotherm is unfavorable.

Dubinin–Radushkevich (DR) isotherm is presented as [27, 34]:

$$ln q_e = ln X_m - \beta.\varepsilon^2 \tag{6}$$

where Xm is the DR monolayer adsorption capacity ($molg^{-1}$), qe (mgg^{-1}) indicates the adsorbed dye per unit weight of adsorbent, β (mol^2J^{-2}) is the constant related with sorption energy and ε is Polanyi potential which is given below as:

$$\varepsilon = R.T.ln\left(1 + \frac{1}{C_e}\right) \tag{7}$$

where T indicates temperature (K), R indicates gas constant (8.314 $Jmol^{-1}K^{-1}$) and Ce indicates the equilibrium concentration of dye (mol L^{-1}). The mean free energy E ($kJmol^{-1}$) was calculated using the following equation:

$$E = \frac{1}{\sqrt{2\beta}}$$ (8)

The calculated parameters were indicated in Table 2.

Brunauer–Emmett–Teller isotherm equation is given as below:

$$\frac{C_e}{(C_i - C_e)q_e} = \frac{1}{Bq_{max\,\square}} + \frac{B-1}{(Bq_{max\,\square})}\left(\frac{C_e}{C_i}\right)$$ (9)

The calculated values, given in Table 2 indicated the Langmuir isotherm is favorable than Freundlich, Brunauer–Emmett–Teller isotherms, and Dubinin–Radushkevich (DR) [34-35]. It is confirmed by high values of R^2 for all samples. It can be also confirmed with RL values. The adsorption is favorable since RL values are between 0 and 1. Langmuir adsorption depicted that the adsorption took place at homogeneous active sites on the adsorbent and adsorbed molecules. And also the results show that the adsorption is monolayer adsorption.

3.5 Thermodynamic

Thermodynamic parameters give information about the feasibility and nature of the adsorption process. Thermodynamic parameters were obtained by given equations to analyze the impact of temperature on the adsorption [36].

$$\Delta G^0 = -RT.\ln 1000 Kd$$ (10)

$$Kd = \frac{q_e}{C_e}$$ (11)

where q_e indicates the amount of adsorbed dye (mg) per L at equilibrium, C_e indicates the equilibrium concentration (mgL^{-1}) of dye in solution, K_d indicates the distribution coefficient for the adsorption.

The enthalpy ($\Delta H°$) change is calculated by the equation:

$$\ln 1000 Kd = -\frac{\Delta H^0}{RT} + \frac{\Delta S^0}{R}$$ (12)

where $R(8.314\ J\ mol^{-1}K^{-1})$ indicates gas constant, $T(K)$ indicates the solution temperature. The calculated thermodynamic parameters were presented in Table 3.

The calculated enthalpy ($\Delta H°$) values of cotton, Cot- KSF, Cot- KSF -chi, and Cot- KSF -chi-MDEU are 7.371, 25.992, 36.091, and 44.860 kJ/mol, respectively. The positive (+) values depict the possibility of physical adsorption and the endothermic reaction [34].

As seen in Table 3 standard free energy $\Delta G°$ values are negatives (-) at all the experimental temperatures. The (-) value of $\Delta G°$ depicts that the RB adsorption is spontaneous for all samples in other words the system doesn't need energy from an external source. As the temperature increase, the $\Delta G°$ values become more negative. On other words, the higher temperature makes the adsorption more spontaneous for all samples [28]. The (+) values $\Delta S°$ of samples suggest the increase in randomness at solution (dye solution) –solid interface (adsorbent) [30, 37, 38].

Table 2. Result of adsorption isotherms at 298 K.

Langmuir $\frac{C_e}{q_e} = \frac{1}{q_mL} + \frac{C_e}{q_m}$		q_{exp} (mg/g)	q_{max} (mg/g)	R_L	R^2
	Cotton	0.17	0.16	n.d	0.997
	Cot- KSF	1.2	1.45	0.16	0.993
	Cot- KSF -chi	2.1	2.22	0.87	0.996
	Cot- KSF -chi -MDEU	3.4	6.38	0.034	0.993
Freundlich $\ln q_e = \ln K_f + \frac{1}{n_f}\ln C_e$		q_{exp} (mg/g)	K_f (mg/g)	n_f	R^2
	Cotton	0.17	0.28	-7.62	0.744
	Cot- KSF	1.2	0.63	5.52	0.931
	Cot- KSF -chi	2.1	1.90	29.59	0.2035
	Cot- KSF -chi -MDEU	3.4	0.48	0.42	0.9917
Dubinin–Radushkevich (DR) isotherm $\ln q_e = \ln X_m - \beta\varepsilon^2$		q_{exp} (mg/g)	X_m (mg/g)	E (kJ/mg)	R^2
	Cotton	0.17	0.17	n.d	0.8372
	Cot- KSF	1.2	1.26	158.11	0.7641
	Cot- KSF -chi	2.1	2.14	707.11	0.0679
	Cot- KSF -chi -MDEU	3.4	3.75	111.80	0.951
Brunauer–Emmett–Teller (BET) $\frac{C_e}{(C_i - C_e)q_e} = \frac{1}{Bq_{max\,\square}} + \frac{B-1}{(Bq_{max\,\square})}\left(\frac{C_e}{C_i}\right)$		q_{exp} (mg/g)	q_{max} (mg/g)	B (J)	R^2
	Cotton	0.17	1.9×10^{-3}	-0,05	0.9182
	Cot-KSF	1.2	0.10	0.47	0.9742
	Cot-KSF -chi	2.1	3.06	0.24	0.571
	Cot-KSF -chi -MDEU	3.4	1.83	0.52	0.7872

Table 3. Thermodynamic parameters of cotton, Cot- KSF, Cot- KSF -chi, and Cot- KSF -chi-MDEU.

T (K) Cotton	ΔG (kJ/mol)	ΔH (kJ/mol)	ΔS (kJ/mol)
298	-2.84		
308	-3.18	7.371	0.034
318	-3.53		
338	-4.21		
T (K) Cot-KSF	ΔG (kJ/mol)	ΔH (kJ/mol)	ΔS (kJ/mol)
298	-8.28		
308	-9.43	25.992	0.115
318	-10.58		
338	-12.88		
T (K) Cot- KSF-chi	ΔG (kJ/mol)	ΔH (kJ/mol)	ΔS (kJ/mol)
298	-9.66		
308	-11.34	36.091	0.154
318	-12.88		
338	-15.961		
T (K) Cot- KSF-chi-MDEU	ΔG (kJ/mol)	ΔH (kJ/mol)	ΔS (kJ/mol)
298	-12.06		
308	-13.97	44.860	0.191
318	-15.88		
338	-19.70		

3.6. Adsorption Kinetics

The impact of contact time on RB adsorption on samples is given in Fig. 6. The adsorptions of RB were studied for 180 min. As can be seen in Fig. 6, 90 min is enough to reach adsorption equilibrium for all samples.
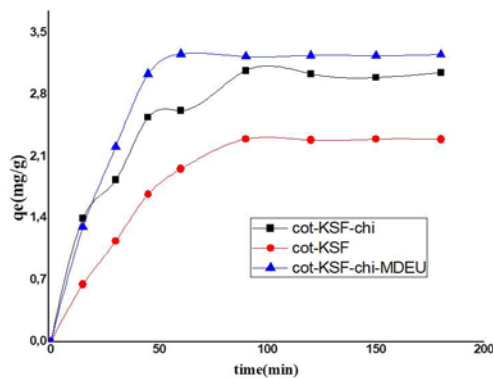
Figure 6. The impact of contact time on adsorption.

The adsorption kinetics gives information about adsorbant-adsorbate interaction. Adsorption capacity and adsorption rate are an essential factors for the selection of the best material to be used in adsorption. The pseudo-first-order and pseudo-second-order are widely used models for adsorption kinetics [3].

Pseudo-first-order kinetic equation is given below:

$$\ln(q_e - q_t) = \ln q_e - k_1 \cdot t \tag{13}$$

where q_e (mgg⁻¹) indicates the adsorbed RB at equilibrium, q_t (mgg⁻¹) indicates the adsorbed RB at any time.
Pseudo-second-order kinetic model equation is:

$$\frac{t}{q_t} = \frac{1}{k_2 \cdot q_e^2} + \frac{t}{q_e} \tag{14}$$

where k_2 (gmg⁻¹min⁻¹) is the pseudo-second-order rate constant.

The initial rate of adsorption was calculated from the given equation:

$$h_{0,2} = k_2 \cdot q_e^2 \tag{15}$$

The half-adsorption time $t_{1/2}$ (min), indicates the required time for the adsorption to take up half equilibrium value.

$$t_{\frac{1}{2}} = \frac{1}{k_2 q_e} \tag{16}$$

Calculated $t_{1/2}$ (min) values are given in Table 4.

Elovich equation is defined as:

$$q_t = \frac{1}{\beta} \cdot \ln(\alpha\beta) + \frac{1}{\beta} \ln t \tag{17}$$

where α (mgg⁻¹min⁻¹) is the initial sorption rate, β (gmg⁻¹) is associated with extending of surface coverage.
Intraparticles diffusion was studied in this project. If the intraparticle diffusion (k_i) (mg/(gmin^{1/2})) is the rate

controlling factor, adsorption of RB varies with the square root of time. And so the adsorption rate can measure by determining the adsorption capacity of adsorbent (q_t) (mg/g) as a function of square root of time ($t^{1/2}$). If the q_t vs $t^{1/2}$ plots go through the origin, intraparticle diffusion is the one rate limiting step. On the other side when the q_t vs $t^{1/2}$ plots don't pass through the origin, it is indicated the boundary layer control (c). And also depict that intraparticle diffusion is not the only rate limiting step [39-42].

Intraparticles diffusion kinetics model is defined with the equation:

$$q_t = k_i \cdot t^{\frac{1}{2}} + c \tag{18}$$

The experimental and computed qe values are close to each other for Elovich equation, Intraparticles diffusion, Pseudo-first-order, and pseudo-second-order kinetic models. And also the correlation coefficients support that RB adsorption system fit for Intraparticles diffusion, Elovich equation, Pseudo-first-order, and pseudo-second-order kinetic models. Based on the correlation coefficients pseudo-second-order kinetic model exhibits a better fit than Pseudo-first-order, Intraparticles diffusion, and Elovich equation kinetic models [20, 29].

Table 4. The results of kinetic studies at 298 K.

The pseudo-second-order		q_{exp} (mg/g)	k (g mg^{-1}min^{-1})	$t_{1/2}$ (min)	h (mg/g.min)	q_e (mg/g)	R^2
	Cot- KSF	2.3	8.41×10^{-3}	29.58	0.136	4.02	0.999
	Cot- KSF -chi	3.1	2.30×10^{-3}	90.91	0.05	4.68	0.996
	Cot- KSF -chi-MDEU	3.2	2.58×10^{-3}	58.82	0.109	6.52	0.998
The pseudo-first-order		q_{exp} (mg/g)	k (s^{-1})	q_e (mg/g)	R^2		
	Cot- KSF	2.3	0.0282	2.54	0.9984		
	Cot- KSF -chi	3.1	0.0283	2.63	0.988		
	Cot- KSF -chi-MDEU	3.2	0.0463	4.12	0.995		
Elovich equation		q_{exp} (mg/g)	α (mg/g.min)	β (g/mg)	R^2		
	Cot-KSF	2.3	0.278	1.086	0.9979		
	Cot-KSF-chi	3.1	0.115	1.089	0.9855		
	Cot-KSF-chi-MDEU	3.2	0.234	0.734	0.9994		
Intra-particle diffusion		q_{exp} (mg/g)	k_i (mg/g.min$^{0.5}$)	C (mg/g)	R^2		
	Cot-KSF	2.3	0.2931	0.3546	0.986		
	Cot-KSF-chi	3.1	0.2960	-0.4801	0.999		
	Cot-KSF-chi-MDEU	3.2	0.5319	-0.7419	0.998		

3.7. Antimicrobial Activity Test

The antibacterial activity of Cot-KSF, Cot-KSF-chi, and Cot-KSF-chi-MDEU was investigated against the *S. Aureus (S.A) and K. Pneumonia (K.P)*. The antibacterial activity results were given in Table 5 and shown by the reduction of bacterial counts. Cot-KSF, Cot-KSF-chi, and Cot-KSF-chi-MDEU show antibacterial activity against the *S.A* and *K.P*. KSF and chitosan have antibacterial activity [43-45]. KSF was used in antibacterial studies. The cationic nature of chitosan inhibits the growth of fungi, yeast, Gram‑positive and Gram‑negative bacteria [43, 45].

In this study KSF and chitosan coated cotton exhibited antibacterial activity against the *S.A* and *K.P*. The best antibacterial activity against *S.A* and *K.P* was investigated for Cot-KSF-chi-MDEU.

Table 5. Antimicrobial activity of Cot-KSF, Cot-KSF-chi, and Cot-KSF-chi-MDEU.

Samples	% Reduction of *S.A*	% Reduction of *K.P*
Cot-KSF	99.99025	99.61429
Cot-KSF-chi	99.775	99.99671
Cot-KSF-chi-MDEU	99.9625	99.99994

4. CONCLUSION

Treated (cot-KSF, Cot-KSF-chi, and Cot-KSF-chi-MDEU) and untreated cotton were fabricated. Results of the characterization were assessed. One-step process of clay-chitosan-based fabrics gained to fabric significantly good properties.

- The treated cotton samples were effectively dyed (free salt) with small quantities of dye. It is economically important for the textile industry. And also, free salt dyeing is an environmentally friendly form of textile dyeing.

- Treated cottons were exhibited antibacterial properties.

- The decomposition temperature of the cotton sample decreased from 369 to 351°C after treatment

- Dye adsorption capacities of cotton samples were investigated. The adsorption of RB on the samples, q_e (mg/g), decreased with the increasing pH value. As the ionic strength increased the dye adsorption capacity of treated cotton samples decreased while untreated samples increased.

- Brunauer–Emmett–Teller, Freundlich, Dubinin-Radushkecich, and Langmuir isotherm equations were studied to investigate the equilibrium character of adsorption. Langmuir isotherm is favorable than Brunauer–Emmett–Teller, Dubinin–Radushkevich (DR), and Freundlich isotherms. The negative value of $\Delta G°$ shows that the RB dye adsorption is spontaneous for all samples. As the temperature increase the $\Delta G°$ values became more negative that showed the adsorption was more spontaneous at higher temperatures for all samples. The positive values $\Delta S°$ of samples suggest the increase in randomness at the solution (dye solution) –solid interface (adsorbent). 90 min is enough to reach adsorption equilibrium for all samples. Related to correlation coefficients, pseudo-second-order kinetic model exhibits a better fit than Elovich equation, Pseudo-first-order, and Intraparticles diffusion kinetic models.

Consequently, clay-chitosan composites can be considered as a hopeful composite for multifunctional finishing textiles. The treatment gained cotton antibacterial properties and easy & salt-free dyeing ability. The ecofriendly treatment can be used in the textile industry. And also treated antibacterial cotton can be used in medical applications.

REFERENCES

1. Periyasamy AP, Venkatesan H. 2018. Eco-materials in textile finishing. Handbook of Ecomaterials. Springer International Publishing, Cham, 1-22.

2. Montaser AS, Mahmoud FA. 2019. Preparation of chitosan-grafted-polyvinyl acetate metal nanocomposite for producing multifunctional textile cotton fabrics. *International Journal of Biological Macromolecules* 124, 659-666.

3. Bharathi KS, Ramesh ST. 2013. Removal of dyes using agricultural waste as low-cost adsorbents: A review. *Applied Water Science* 3(4), 773-790.

4. Montazer M, Malek RMA, Rahimi A. 2007. Salt free reactive dyeing of cationized cotton. *Fibers and Polymers* 8(6), 608-612.

5. Kant R. 2011. Textile dyeing industry an environmental hazard. *Natural Science* 4(1), 22-26.

6. Kadam AA, Lee DS. 2015. Glutaraldehyde cross-linked magnetic chitosan nanocomposites: Reduction precipitation synthesis, characterization, and application for removal of hazardous textile dyes. *Bioresource technology* 193, 563-567.

7. Singha K, Maity S, Singha M. 2012. The salt-free dyeing on cotton: An approach to effluent free mechanism; can chitosan be a potential option. *International Journal of Textile Science* 1(6), 69-77.

8. Sharma P, Kaur H, Sharma M, Sahore V. 2011. A review on applicability of naturally available adsorbents for the removal of hazardous dyes from aqueous waste. *Environmental Monitoring and Assessment* 183(1-4), 151-195.

9. Kausar A, Iqbal M, Javed A, Aftab K, Bhatti H N, Nouren S. 2018. Dyes adsorption using clay and modified clay: A review. *Journal of Molecular Liquids* 256, 395-407.

10. Rehan M, El-Naggar ME, Mashaly HM, Wilken R. 2018. Nanocomposites based on chitosan/silver/clay for durable multi-functional properties of cotton fabrics. *Carbohydrate Polymers* 182, 29-41.

11. Reddy DHK, Lee SM. 2013. Application of magnetic chitosan composites for the removal of toxic metal and dyes from aqueous solutions. *Advances in Colloid and Interface Science* 201, 68-93.

12. Wang Q, Chen W, Zhang Q, Ghiladi RA, Wei Q. 2018. Preparation of photodynamic P (MMA-co-MAA) composite nanofibers doped with MMT: A facile method for increasing antimicrobial efficiency. *Applied Surface Science* 457, 247-255.

13. Arık B, Seventekin N. 2011. Evaluation of antibacterial and structural properties of cotton fabric coated by chitosan/titania and chitosan/silica hybrid sol-gel coatings. *Tekstil ve Konfeksiyon* 21(2), 107-115.

14. Tursucular O, Cerkez İ, Orhan M, Aykut Y. 2018. Preperation and antibacterial investigation of polycaprolactone/chitosan nano/micro fibers by using different solvent systems. *Tekstil ve Konfeksiyon* 28(3), 221-228.

15. Chung YC, Wang HL, Chen YM, Li SL. 2003. Effect of abiotic factors on the antibacterial activity of chitosan against waterborne pathogens. *Bioresource Technology* 88(3), 179-184.

16. Cao C, Xiao L, Chen C, Shi X, Cao Q, Gao L. 2014. In situ preparation of magnetic Fe_3O_4/chitosan nanoparticles via a novel reduction–precipitation method and their application in adsorption of reactive azo dye. *Powder Technology* 260, 90-97.

17. Yu C. 2016. Preparation and Application of the Composite from Chitosan. Handbook of Composites from Renewable Materials, Structure and Chemistry 1, 371.

18. Lavorgna M, Attianese I, Buonocore GG, Conte A, Del Nobile MA, Tescione F, Amendola E. 2014. MMT-supported Ag nanoparticles for chitosan nanocomposites: structural properties and antibacterial activity. *Carbohydrate Polymers* 102, 385-392.

19. Altınışık A, Bozacı E, Akar E, Seki Y, Yurdakoc K, Demir A, Özdogan E. 2013. Development of antimicrobial cotton fabric using bionanocomposites. *Cellulose* 20(6), 3111-3121.

20. Akar E, Altinişik A, Seki Y. 2013. Using of activated carbon produced from spent tea leaves for the removal of malachite green from aqueous solution. *Ecological Engineering* 52, 19-27.

21. Li R, Liu C, Ma J, Yang Y, Wu H. 2011. Effect of org-titanium phosphonate on the properties of chitosan films. *Polymer Bulletin* 67(1), 77-89.

22. Kang S, Qin L, Zhao Y, Wang W, Zhang T, Yang L, Song S. 2020. Enhanced removal of methyl orange on exfoliated montmorillonite/chitosan gel in presence of methylene blue. *Chemosphere* 238, 124693.

23. Kaur K, Jindal R. 2019. Self-assembled GO incorporated CMC and Chitosan-based nanocomposites in the removal of cationic dyes. *Carbohydrate Polymers* 225, 115245.

24. Abdurrahim I. 2019. Water sorption, antimicrobial activity, and thermal and mechanical properties of chitosan/clay/glycerol nanocomposite films. *Heliyon* 5(8), e02342.

25. Gaan S, Sun G. 2009. Effect of nitrogen additives on thermal decomposition of cotton. *Journal of Analytical and Applied Pyrolysis* 84(1), 108-115.

26. Ouajai S, Shanks RA. 2005. Composition, structure and thermal degradation of hemp cellulose after chemical treatments. *Polymer Degradation and Stability* 89(2), 327-335.

27. Çelebi M, Özdemir Z. 2017. Dyestuffs removal from synthetic wastewater with chitosan, cross-linked chitosan and chitosan-poly (acrylic acid) conjugate. *Tekstil ve Konfeksiyon* 27(3), 283-288.

28. Hwang SY, Yoo ES, Im SS. 2009. Effect of the urethane group on treated clay surfaces for high-performance poly (butylene succinate)/montmorillonite nanocomposites. *Polymer Degradation and Stability* 94(12), 2163-2169.

29. Chen D, Chen J, Luan X, Ji H, Xia Z. 2011. Characterization of anion–cationic surfactants modified montmorillonite and its

30. Newcombe G, Drikas M. 1997. Adsorption of NOM onto activated carbon: electrostatic and non-electrostatic effects. *Carbon* 35(9), 1239-1250.

31. Alberghina G, Bianchini R, Fichera M, Fisichella S. 2000. Dimerization of Cibacron Blue F3GA and other dyes: influence of salts and temperature. *Dyes and Pigments* 46(3), 129-137.

32. Germán-Heins J, Flury M. 2000. Sorption of Brilliant Blue FCF in soils as affected by pH and ionic strength. *Geoderma* 97(1-2), 87-101.

33. Ali I, Alothman Z A, Alwarthan A. 2017. Uptake of propranolol on ionic liquid iron nanocomposite adsorbent: kinetic, thermodynamics and mechanism of adsorption. *Journal of Molecular Liquids* 236, 205-213.

34. Konicki W, Aleksandrzak M, Moszyński D, Mijowska E. 2017. Adsorption of anionic azo-dyes from aqueous solutions onto graphene oxide: equilibrium, kinetic and thermodynamic studies. *Journal of Colloid and Interface Science* 496, 188-200.

35. Akram M, Bhatti HN, Iqbal M, Noreen S, Sadaf S. 2017. Biocomposite efficiency for Cr (VI) adsorption: Kinetic, equilibrium and thermodynamics studies. *Journal of Environmental Chemical Engineering* 5(1), 400-411.

36. Milonjić SK. 2007. A consideration of the correct calculation of thermodynamic parameters of adsorption. *Journal of the Serbian Chemical Society* 72(12), 1363-1367.

37. Bedin KC, Martins AC, Cazetta AL, Pezoti O, Almeida VC. 2016. KOH-activated carbon prepared from sucrose spherical carbon: Adsorption equilibrium, kinetic and thermodynamic studies for Methylene Blue removal. *Chemical Engineering Journal* 286, 476-484.

38. Tran HN, You SJ, Chao HP. 2016. Thermodynamic parameters of cadmium adsorption onto orange peel calculated from various methods: A comparison study. *Journal of Environmental Chemical Engineering* 4(3), 2671-2682.

39. Belaroussi A, Labed F, Khenifi A, Akbour RA, Bouberka Z, Kameche M, Derriche Z. 2018. A novel approach for removing an industrial dye 4GL by an Algerian Bentonite. *Acta Ecologica Sinica* 38(2), 148-156.

40. Weber WJ, Morris JC. 1963. Kinetics of adsorption on carbon from solution. *Journal of the Sanitary Engineering Division* 89(2), 31-60.

41. Juang RS, Wu FC, Tseng RL. 2000. Mechanism of adsorption of dyes and phenols from water using activated carbons prepared from plum kernels. *Journal of Colloid and Interface Science* 227(2), 437-444.

42. Ho YS, McKay G. 1999. Pseudo-second order model for sorption processes. *Process Biochemistry* 34(5), 451-465.

43. Ignatova M, Manolova N, Rashkov I. 2013. Electrospun Antibacterial Chitosan-B ased Fibers. *Macromolecular Bioscience* 13(7), 860-872.

44. Maryan AS, Montazer M, Rashidi A, Rahimi MK. 2013. Antibacterial properties of clay layers silicate: a special study of montmorillonite on cotton fiber. *Asian Journal of Chemistry* 25(5), 2889.

45. Demir A, Öktem T, Seventekin N. 2008. Investigation of the usage of chitosan as an antimicrobial agent in textile industry. *Tekstil ve Konfeksiyon* 18(2), 94-102.